JVI Journals.ASM.org

The Level of Viral Infection of Antigen-Presenting Cells Correlates with the Level of Development of Theiler's Murine Encephalomyelitis Virus-Induced Demyelinating Disease

Young Hee Jin,[a]* Hyun Seok Kang,[a] Wanqiu Hou,[a]* Liping Meng,[a] Byung S. Kim[a,b]

Department of Microbiology-Immunology[a] and Department of Pathology,[b] Northwestern University Medical School, Chicago, Illinois, USA

ABSTRACT

Intracerebral infection with Theiler's murine encephalomyelitis virus (TMEV) induces immune-mediated demyelinating disease in susceptible SJL/J mice but not in resistant C57BL/6 mice. Previous studies have indicated that the major histocompatibility complex (MHC) genes play the most prominent role in the development of TMEV-induced demyelinating disease. In this study, we used C57BL/6.S (B6.S) congenic mice, which carry *H-2*^{s} MHC genes instead of *H-2*^{b} MHC genes in conjunction with the C57BL/6 (B6) background genes. Our data show that virus-infected B6.S mice are free from disease and have significantly lower viral loads than susceptible SJL mice, particularly in the spinal cord. A strong protective Th1-type T helper response with virtually no pathogenic Th17 response was detected in B6.S mice, in contrast to the reduced Th1- and robust Th17-type responses in SJL mice. Notably, lower levels of viral infectivity in B6.S antigen-presenting cells (APCs) correlated with the disease resistance and T-cell-type response. *In vitro* studies using APCs from B6.S and SJL mice show that TLR2, -3, -4, and -7, but not TLR9, signaling can replace viral infection and augment the effect of viral infection in the differentiation of the pathogenic Th17 cell type. Taken together, these results strongly suggest that the viral replication levels in APCs critically affect the induction of protective versus pathogenic Th cell types via the signaling of pattern recognition receptors for innate immune responses. Our current findings further imply that the levels of viral infectivity/replication and TLR-mediated signaling play critical roles in the pathogenesis of chronic viral diseases.

IMPORTANCE

This study indicates that innate immune cytokines produced in antigen-presenting cells stimulating the T cell immune responses during early viral infection play a critical role in determining the susceptibility of mice to the development of demyelinating disease. The level of innate immune cytokines reflects the level of initial viral infection in the antigen-presenting cells, and the level determines the development of T cell types, which are either protective or pathogenic. The level of initial viral infection to the cells is controlled by a gene or genes that are not associated with the major histocompatibility antigen complex genes. This finding has an important implication in controlling not only chronic viral infections but also infection-induced autoimmune-like diseases, which are closely associated with the pathogenic type of T cell responses.

Intracerebral infection of susceptible mice with Theiler's murine encephalomyelitis virus (TMEV) induces an immune-mediated, progressive inflammatory demyelinating disease (IDD) that is similar to a progressive form of human multiple sclerosis (MS) (1, 2). Histopathology and clinical similarities between TMEV-induced disease and human disease make this a relevant model to investigate the mechanisms underlying demyelinating diseases (3).

Different inbred mouse strains exhibit different levels of susceptibility to the demyelinating disease induced by TMEV (TMEV-IDD). For example, SJL/J (*H-2*^{s}), SWR (*H-2*^{q}), RIII (*H-2*^{r}), PL/J (*H-2*^{u}), and DBA/2 (*H-2*^{d}) mice are highly susceptible, AKR/J (*H-2*^{k}) and C3H/J (*H-2*^{k}) mice are moderately susceptible, and C57BL/6 (*H-2*^{b}), C57BL/10 (*H-2*^{b}), and BALB/c (*H-2*^{d}) mice are resistant to the development of demyelinating disease (4). One of the most important susceptibility loci is linked to the *H-2D* gene complex (5, 6). In addition, a locus on chromosome 6 near the *Tcrb* locus and a locus on chromosome 3 were identified as susceptibility-linked loci for the development of demyelinating disease (7, 8). However, the viral persistence level in the central nervous system (CNS) is associated with a locus on chromosome 10, a locus (or possible two loci) on chromosome 14, and a locus on chromosome 18 (9–11). Nevertheless, SJL/J (SJL) mice represent a prototypical susceptible mouse strain and C57BL/6 (B6) mice represent a prototypical resistant mouse strain for both viral persistence and the development of demyelinating disease (4, 12). SJL

Received 26 August 2014 **Accepted** 19 November 2014

Accepted manuscript posted online 26 November 2014

Citation Jin YH, Kang HS, Hou W, Meng L, Kim BS. 2015. The level of viral infection of antigen-presenting cells correlates with the level of development of Theiler's murine encephalomyelitis virus-induced demyelinating disease. J Virol 89:1867–1878. doi:10.1128/JVI.02471-14.

Editor: S. Perlman

Address correspondence to Byung S. Kim, bskim@northwestern.edu.

Y.H.J., H.S.K., and W.H. contributed equally to this article.

* Present address: Young Hee Jin, Laboratory of Immune Regulation, Department of Biomedical Sciences, Seoul National University College of Medicine, Seoul, South Korea; Wanqiu Hou, Division of Dermatology, Department of Medicine, David Geffen School of Medicine at University of California at Los Angeles, Los Angeles, California, USA.

doi:10.1128/JVI.02471-14

mice are predisposed to viral persistence in the CNS and are highly susceptible to developing demyelinating disease, whereas B6 mice clear viral infection within 2 to 4 weeks and remain free of disease (12). Hence, it appears that viral persistence is well correlated with disease in these mouse strains (13).

Early genetic studies have demonstrated that the *H-2D*^{b} gene is critical for resistance to TMEV-induced demyelinating disease, because transgenic (Tg) expression of *H-2D*^{b} in susceptible FVB mice rendered them resistant (14). Therefore, CD8$^+$ T cells restricted to the *H-2D* haplotype seem to be an important mediator of protection and/or pathogenesis. Surprisingly, F1 (*H-2*$^{b/s}$) B6 and SJL mice preferentially developed *H-2D*^{b}-restricted CD8$^+$ T cells, not the *H-2K*^{s}-restricted CD8$^+$ T cells found in SJL/J mice (15). Thus, it is conceivable that F1 mice clear virus efficiently using the *H-2D*^{b}-restricted CD8$^+$ T cells. If major histocompatibility complexes (MHCs) and their restricted CD8$^+$ T cells primarily determine the susceptibility to disease, B6.S mice bearing *H-2*^{s} would be susceptible to TMEV-IDD.

In contrast to the virus-clearing CD8$^+$ T cell responses, CD4$^+$ T cell responses are thought to play an important role in the pathogenesis of demyelinating disease and many other autoimmune diseases (16–18). Numerous earlier studies reported that Th1 cells play a decisive pathogenic role in the development of demyelinating disease in susceptible mice (19–21). However, our recent reports show that Th17 responses, which are preferentially generated in susceptible mice, such as SJL/J mice (*H-2*^{s}), are strongly implicated in pathogenesis. For example, when interleukin-17 (IL-17) was neutralized by anti-IL-17 monoclonal antibodies, SJL/J mice were protected from disease (18). On the contrary, Th1 responses are preferentially generated in resistant mice, such as B6 (*H-2*^{b}) and F1 (*H-2*$^{b/s}$) SJL and B6 mice; these Th1 responses provide protection from demyelinating disease (15).

In this study, we investigated the underlying immunological mechanisms associated with viral persistence in the CNS and the development of demyelinating disease using susceptible SJL (*H-2*^{s}) mice and resistant B6.S (*H-2*^{s}) mice, which carry the background genes of B6 mice in conjunction with the *H-2* genes of susceptible SJL mice. In this study, we used B6.S congenic mice carrying *H-2*^{s} MHC genes, which are the same as those in the susceptible SJL mice, rather than the *H-2*^{b} MHC genes found in resistant B6 mice. Following TMEV infection in these mice, the epitope specificities of the CD4$^+$ and CD8$^+$ T cells would be expected to be the same as those in SJL mice. Thus, this mouse strain permits us to investigate the effects of genes on T cell responses (or signaling pathways) other than MHC genes. Our present data show that B6.S mice are free from disease, and CD4$^+$ T cells preferentially differentiate into protective Th1 cells rather than pathogenic Th17 cells through an intrinsic property of antigen-presenting cells (APCs) residing in resistant mice. Notably, *in vitro* differentiation studies of identical T cell receptor-transgenic (TCR-Tg) T cells using bone-marrow-derived dendritic cells (BMDCs) from B6.S and SJL mice show that the viral infectivity level in the APCs correlates with the development of a pathogenic Th17 response. Pattern recognition receptors, such as Toll-like receptor 2 (TLR2), -3, -4, and -7, but not TLR9, similarly enhance the level of Th17 differentiation in the absence or presence of viral infection. Taken together, these results strongly suggest that viral replication levels in APCs critically affect the induction of protective versus pathogenic Th types via the consequent innate immune responses. Present data also suggest that genes other than those in the MHC are critically involved in the initial viral load levels of APCs and the consequent outcome of clinical disease.

MATERIALS AND METHODS

Animals. Female SJL/J (SJL) and C57BL/6 (B6) mice were purchased from Charles River Laboratories (Charles River, MA) through the National Cancer Institute (Frederick, MD). Female B6.SJL-*H2*^{S}*C3*^{C}/1CyJ (B6.S) mice were purchased from Jackson Laboratory (Bar Harbor, ME). The generation of VP2-TCR-Tg transgenic mice was previously described (18), and this strain (018030 SJL.Cg-Tg(TcraTcrbVP2)1Bkim/J) can be obtained from Jackson Laboratory. All mice were housed at the Center for Comparative Medicine Facility of Northwestern University. Experimental procedures approved by the Northwestern University Animal Care and Use Committee (ACUC) were used in accordance with NIH animal guidelines.

Reagents. Synthetic peptides were purchased from Genmed Synthesis (San Francisco, CA). All peptide stocks (2 mM) were prepared in 8% dimethyl sulfoxide in phosphate-buffered saline (PBS). All antibodies used for flow cytometry were purchased from BD Pharmingen (San Diego, CA). Anti-mouse IL-6 antibody (Invitrogen), anti-IL-12p40 antibody (eBioscience), and 100 ng/ml IL-17 (PeproTech) were used. TLR2 ligands Pam3CSK4 (Pam) and lipoteichoic acid (LTA) (from *Staphylococcus aureus*) were obtained from InvivoGen (San Diego, CA) and used at 10 ng/ml and 1 μg/ml, respectively. The TLR3 ligand poly(I:C) was obtained from Calbiochem (La Jolla, CA) and used at 50 μg/ml. The TLR4 ligand lipopolysaccharide (LPS) (*Escherichia coli* O111:B4) was obtained from Sigma (St. Louis, MO) and used at 100 ng/ml. The TLR7 ligand CL087 and the TLR9 ligand type B CpG oligonucleotide were obtained from InvivoGen (San Diego, CA) and used at 0.1 μg/ml and 10 μg/ml, respectively.

TMEV propagation and infection of mice. The BeAn strain of TMEV was propagated and the titer determined in BHK cells grown in Dulbecco's modified Eagle medium (DMEM) supplemented with 7.5% donor calf serum. For intracerebral (i.c.) infection, 30 μl (approximately 1×10^6 PFU) of TMEV BeAn was injected into the right cerebral hemisphere of 6- to 8-week-old mice anesthetized with isoflurane. Clinical symptoms of disease were assessed weekly on the following grading scale: grade 0, no clinical signs; grade 1, mild waddling gait; grade 2, moderate waddling gait and hind-limb paresis; grade 3, severe hind-limb paralysis; grade 4, severe hind-limb paralysis and loss of righting reflex; and grade 5, death.

Plaque assays. After perfusion with Hanks' balanced salt solution (HBSS), brains and spinal cords were removed from virus-infected mice and homogenized through a wire mesh. The tissue homogenate was used to perform standard plaque assays on a BHK-21 cell monolayer (22). The plaques were visualized after fixation with methanol and staining with 0.1% crystal violet.

Histopathological staining. At 85 days postinfection with TMEV, mice were perfused via intracardiac puncture with 50 ml of phosphate-buffered saline (PBS). Brains and spinal cords from mice were dissected, fixed in 4% formalin in PBS for 4 days, transferred to 30% sucrose–PBS solution for another 24 h, and embedded in paraffin for sectioning and staining. Paraffin-processed brains and spinal cords were sectioned at 6 μm. Three sets of adjacent sections from each animal were deparaffinized, rehydrated, and evaluated separately after staining with Luxol Fast Blue (LFB) for axonal demyelination, hematoxylin and eosin (H&E) for inflammatory infiltrates, and Bielschowsky silver stain for axon damage and loss. Sections were observed and recorded using a Leica DMR microscope, and the images were captured using an AxioCam MRc camera and AxioVision imaging software.

Isolation of CNS-infiltrating lymphocytes. Mice were perfused through the left ventricle with 30 ml of sterile Hanks' balanced salt solution (HBSS). Excised brains and spinal cords were forced through wire mesh and incubated at 37°C for 45 min in 250 μg/ml of collagenase type 4 (Worthington Biochemical Corp., Lakewood, NJ). CNS-infiltrating lymphocytes were then enriched at the bottom 1/3 of a continuous Percoll (Pharmacia, Piscataway, NJ) gradient after centrifugation for 30 min at

27,000 × *g*. For the cell analysis, the Fc receptors of the isolated CNS cells were blocked using 50 μl of 2.4G2 hybridoma (ATCC) supernatant by incubation at 4°C for 30 min. The cells were stained with anti-CD8 (clone 53-6.7), anti-CD4 (clone GK1.5), anti-CD11b (clone M1/79), anti-CD45 (clone 30-F11), or anti-CD45.1 (clone A20) antibodies. All cells were analyzed using a Becton Dickinson LSRII flow cytometer (BD) and FlowJo software (Treestar).

T cell proliferation assay. Splenocytes (1×10^6 cells/well) from infected mice were stimulated with the indicated stimuli in 96-well flat-bottom microtiter plates for 48 h, pulsed with 1.0 μCi [^{3}H]TdR for 18 h and then harvested. Measurements of [^{3}H]TdR uptake by the cells were determined in triplicate and expressed as net counts per minute (Δcpm ± standard error of the mean [SEM]) after subtraction of the background count of cultures with PBS.

Measurement of cytokine levels. The cytokine levels produced by splenocytes (1×10^6 cells/well) from TMEV-infected mice were assessed by enzyme-linked immunosorbent assay (ELISA) after the indicated stimulations. Gamma interferon (IFN-γ) (OPTEIA kit; BD Pharmingen) and IL-17 (R&D Systems) levels were measured using the respective cytokine-specific ELISA systems. The values are expressed as the mean ± standard deviation of values from triplicate samples.

Real-time PCR. Total RNA was isolated by TRIzol (Invitrogen) and reverse transcribed to cDNA using Moloney murine leukemia virus reverse transcriptase (Invitrogen). The cDNAs were amplified with specific primer sets in SYBR green master mix using an iCycler (Bio-Rad). The sense and antisense primer sequences are as follows: TMEV (VP1), 5′-TGACTAAGCAGGACTATGCCTTCC-3′ and 5′-CAACGAGCCACATATGCGGATTAC-3′; IFN-γ, 5′-ACTGGCAAAAGGATGGTGAC-3′ and 5′-TGAGCTCATTGAATGCTTGG-3′; IL-17A, 5′-GGGGATCCATGAGTCCAGGGAGAGC-3′ and 5′-CCCTCGAGTTAGGCTGCCTGGCGGA-3′; and glyceraldehyde-3-phosphate dehydrogenase (GAPDH), 5′-AACTTTGGCATTGTGGAAGGGCTC-3′ and 5′-TGCCTGCTTCACCACCTTCTTGAT-3′. GAPDH expression served as an internal reference for normalization. Real-time PCR was performed in triplicate.

Generation of bone marrow-derived DCs. Bone marrow cells were harvested from the femurs and tibias of adult mice and cultured in RPMI medium supplemented with 10% fetal bovine serum (FBS) and 20 ng/ml murine recombinant granulocyte-macrophage colony-stimulating factor (rGM-CSF) (PeproTech) for 5 days as described previously (23).

TMEV infection of DCs. BMDCs were incubated with TMEV for 1 h at room temperature with intermittent shaking in RPMI with 0.1% bovine serum albumin, washed twice, and resuspended in RPMI containing 10% FBS and 20 ng/ml murine rGM-CSF at the indicated multiplicity of infection (MOI) and incubation time. After an additional 4 h of incubation with Golgi-Plug (BD), the cells were fixed, permeabilized with Cytofix/Cytoperm (BD Bioscience), blocked with 1% normal goat serum (Invitrogen), and stained with an anti-TMEV monoclonal antibody (8C). The cells were then stained with anti-CD11c (clone HL3) antibody and analyzed on a flow cytometer.

Detection of intracellular cytokines. To measure the virus antigen-specific response of CNS-infiltrating mononuclear cells, freshly isolated cells from the CNS were cultured in 96-well round-bottom plates in the presence of 2 μM the indicated viral peptides and 0.7 μg/ml GolgiStop (BD) for 6 h at 37°C. The cells were then incubated in 50 μl of 2.4G2 hybridoma (ATCC) supernatant for 30 min at 4°C to block the Fc receptors. Allophycocyanin-conjugated anti-CD8 (clone 53-6.7) antibody or allophycocyanin-conjugated anti-CD4 (clone L3T4) antibody was added, and the cells were incubated for an additional 30 min at 4°C. After two washes, intracellular IFN-γ or IL-17 staining was performed with allophycocyanin-labeled rat monoclonal anti-IFN-γ (XMG1.2) or anti-IL-17 (TC11-18H10) antibody using a Cytofix/Cytoperm kit (BD Bioscience) according to the manufacturer's instruction. The cells were analyzed using a flow cytometer. For the assessment of IFN-γ and IL-17 production by VP2-TCR-Tg CD4$^+$ T cells, CD4$^+$ T cells were isolated from VP2-TCR-Tg SJL mice by positive immunomagnetic cell sorting (Miltenyi Biotec) and primed with PBS, 2 μM $VP2_{74-86}$ peptide, and 1 μg/ml UV-inactivated TMEV (UV-TMEV)-treated or TMEV-infected SJL or B6.S BMDCs with or without the indicated cytokines, antibodies, or TLR agonists for 4 days. To induce sustaining production of cytokines by antigen-differentiated T cells, the cultures were restimulated with 50 ng/ml phorbol myristate acetate (PMA) (Sigma) and 1 ng/ml ionomycin (Sigma) for 6 h in the presence of GolgiStop and stained with allophycocyanin-labeled rat monoclonal anti-IFN-γ (XMG1.2) antibody or phycoerythrin (PE)-labeled rat monoclonal anti-IL-17 (TC11-18H10) antibody and fluorescein isothiocyanate (FITC)-conjugated anti-CD4 (clone L3T4) antibody. The levels and proportions of cytokine-producing cells were analyzed using flow cytometry.

Statistical analyses. The significance of the differences (two-tailed *P* value) between experimental groups was analyzed with an unpaired Student's *t* test using the InStat program (GraphPad Software, San Diego, CA). Values of $P < 0.05$ were considered to be significant. For multigroup comparisons, a one-way analysis of variance (ANOVA) with a Tukey-Kramer multiple-comparison test was used.

RESULTS

B6.S mice infected with TMEV do not develop demyelinating disease. B6.S mice have the B6 background genes but share the MHC *H-2*^{s} genes of TMEV-susceptible SJL mice. To examine the disease susceptibility of B6.S mice, we monitored the development of clinical signs following intracerebral TMEV infection for 85 days (Fig. 1A). Susceptible SJL mice ($n = 10$) started to develop clinical signs at day 21, with 90% of the population showing clinical signs at day 35, whereas none of the TMEV-infected B6.S mice ($n = 10$) showed symptoms at either time point. We further examined the virus levels in the brains and spinal cords of the mice at 8, 21, and 85 days postinfection (dpi) using a plaque assay (Fig. 1B). The viral levels in the spinal cords were significantly lower in B6.S mice throughout the time period than those in susceptible SJL mice. However, the viral loads in the brains were inconsistent: drastically higher (100-fold) in B6.S mice at 8 dpi and less than 2-fold higher at 85 dpi but significantly lower (>20-fold) at 21 dpi. These results suggest that the initial viral load in the brain in B6.S mice is higher than that in SJL mice, and the viral load in B6.S mice is more efficiently cleared, although unlike B6 mice, these mice fail to completely clear the virus. In contrast, the viral load in the spinal cord in B6.S mice was lower than in SJL mice throughout the time course. It is unclear at this time whether the lower viral load in the spinal cord of B6.S mice reflects the lower trafficking of the virus to the spinal cord, lower viral replication, or higher viral clearance in the spinal cord.

To correlate the levels of clinical disease development (Fig. 1) to the demyelination process in the CNS of TMEV-infected SJL and B6.S mice, histopathologic examinations were performed at 85 dpi (Fig. 2). More severe demyelination, higher cellular infiltration, and greater axonal loss were observed both in the brains (not shown) and spinal cords of SJL mice compare to B6.S mice (Fig. 2). Bielschowsky silver staining, which stains axons black, was used to evaluate axonal loss. There was larger vacuolation and severe axonal loss in the demyelinated regions of the spinal cords of SJL mice compared to B6.S mice (Fig. 2A). LFB staining, which stains myelin blue, revealed much higher demyelination in the SJL spinal cords compared to the B6.S spinal cords (Fig. 2A and B). H&E staining showed numerous inflammatory cells in both the demyelinated and the intact regions of the spinal cords of SJL mice, but these cells were barely evident in B6.S mice (Fig. 2A and B). These data suggest that B6.S mice reduce viral loads in the CNS

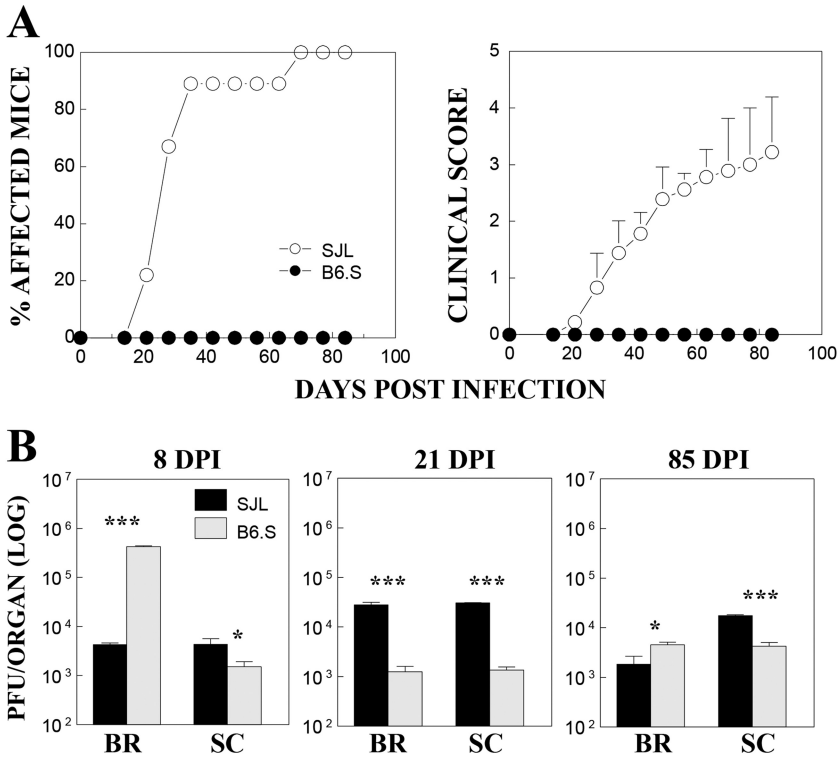

FIG 1 Development of TMEV-induced demyelinating disease and viral loads in the CNS of TMEV-infected SJL mice and B6.S mice. (A) The frequency and severity of demyelinating disease in TMEV-infected SJL mice ($n = 10$) and B6.S mice ($n = 10$) were monitored for 85 days after TMEV infection. (B) Viral persistence levels in the brains (BR) and spinal cords (SC) of infected mice at 8, 21, and 85 days postinfection (DPI) were determined by plaque assay. Data represent values from a representative experiment from three independent experiments conducted with CNS pools of three mice per group. The values given are means ± standard deviations of results from triplicate analyses. Statistically significant differences among the groups at a given time point are indicated with asterisks (*, $P < 0.05$; ***, $P < 0.001$).

more efficiently than SJL mice, causing less cellular infiltration and axonal loss, which leads to resistance to the development of TMEV-IDD.

T cell responses to TMEV epitopes are higher in B6.S mice than in SJL mice. Because CNS-infiltrating T cell responses in the first few weeks of TMEV infection are involved in the protection and/or pathogenesis of demyelinating disease, we compared the levels of $CD4^+$ and $CD8^+$ T cells accumulated in the CNS of infected SJL and B6.S mice at 8 and 21 dpi (Fig. 3A). The proportion of $CD4^+$ T cells in the CNS of B6.S mice was slightly lower than that of the susceptible SJL mice. In contrast, the proportion of $CD8^+$ T cells in the CNS of B6.S mice was higher than that of the susceptible SJL mice. These results suggest that the relatively lower proportion of $CD4^+$ T cells and higher proportion of $CD8^+$ T cells contribute to resistance to the development of demyelinating disease in B6.S mice. However, the overall $CD4^+$ [$(8.9 \pm 4.3) \times 10^5$ versus $(7.2 \pm 1.7) \times 10^5$] and $CD8^+$ [$(3.8 \pm 0.9) \times 10^5$ versus $(3.5 \pm 0.3) \times 10^5$] T cell numbers infiltrating the CNS were similar in SJL and B6S mice at 8 dpi.

We previously reported that high levels of IFN-γ-producing $CD4^+$ Th1 cells in the CNS of TMEV-infected mice play a protective role, whereas IL-17-producing Th17 cells contribute to the pathogenesis of demyelinating disease (18, 24). To further compare the levels of protective $CD4^+$ and $CD8^+$ T cells in the CNS of TMEV-infected SJL and B6.S mice, the proportions and numbers of IFN-γ-producing $CD4^+$ and $CD8^+$ T cells were assessed at 8 and 21 days postinfection following the stimulation of CNS-infiltrating cells with a mixture of $I\text{-}A^s$-restricted structural capsid epitope peptides (SP: $VP1_{233–250}$, $VP2_{74–86}$, and $VP3_{24–37}$), nonstructural epitope peptides (NSP: $3D_{6–23}$, $3D_{21–36}$, and $3D_{412–430}$) or $H\text{-}2K^s$-restricted CD8 epitope peptides ($VP3_{159–166}$, $VP3_{173–181}$ and $VP1_{11–20}$). B6.S mice had significantly higher proportions of Th1 responses to both SP and NSP epitopes compared to SJL mice at 8 and 21 dpi (Fig. 3B). However, the proportions of TMEV-specific $CD8^+$ T cell responses were similar in the CNS of virus-infected B6.S mice and SJL mice (Fig. 3C). The overall numbers of IFN-γ-producing $CD4^+$ T cells in the CNS of virus-infected resistant B6.S mice were also significantly higher, particularly at 8 dpi, compared to the susceptible SJL mice (Fig. 3D). In contrast, the number of virus-specific $CD8^+$ T cells in the CNS of B6.S mice was lower than that in SJL mice at 8 dpi and indifferent at 21 dpi. Therefore, the overall levels of protective virus-specific $CD4^+$ T cell responses, but not of $CD8^+$ T cell responses, in the CNS of TMEV-infected B6.S mice are significantly higher than those in the CNS of SJL mice.

Levels of peripheral $CD4^+$ and $CD8^+$ T cell responses of SJL and B6.S mice infected with TMEV were also assessed at 8 and 21 dpi (Fig. 4). Splenic $CD4^+$ T cells from B6.S mice proliferated significantly less in response to $I\text{-}A^s$-restricted SP and NSP epitopes compared to SJL mice at 8 dpi. However, these T cells from B6.S mice produced significantly higher levels of IFN-γ in response to NSP but lower levels of IFN-γ in response to SP compared to SJL $CD4^+$ T cells. IFN-γ levels produced by B6.S $CD8^+$ T cells were also higher than those produced by SJL $CD8^+$ T cells at

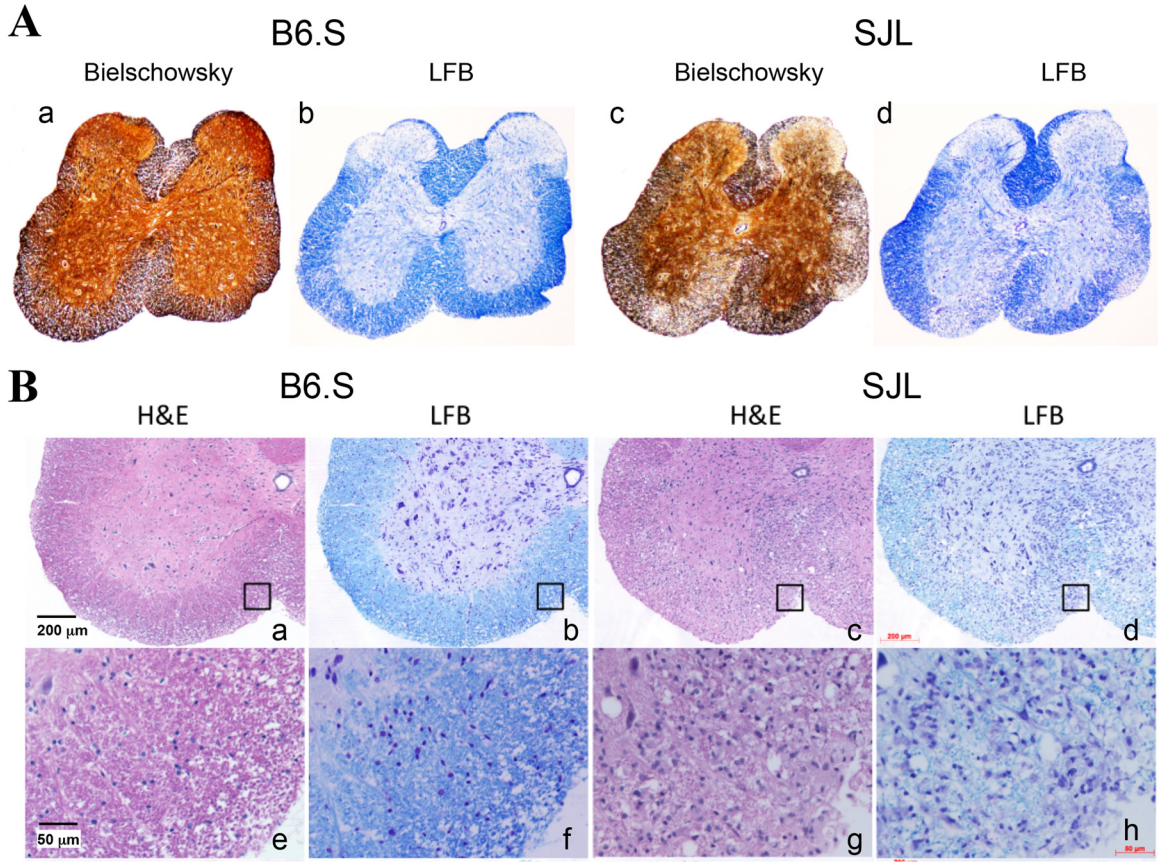

FIG 2 Histopathological changes in the spinal cords of TMEV-infected B6.S and SJL mice at 85 days postinfection. (A) Bielschowsky silver staining and LFB staining showed very minor axonal loss and demyelination, respectively, in the spinal cords of B6.S mice (a and b), in contrast to marked axonal loss and demyelination in the spinal cords of SJL mice (c and d). (B) Minimal infiltration is shown in the spinal cord of B6.S mice (a and b), based on H&E or LFB staining, in contrast to numerous infiltrating lymphocytes/monocytes in the spinal cords of SJL mice (c and d). Higher magnifications of the indicated squares in panels a, b, c, and d are shown in panels e, f, g, and h, respectively.

8 dpi. These higher IFN-γ responses by B6.S mice were decreased to levels lower than those by SJL mice at 21 dpi. The reduction in IFN-γ production at 21 dpi is consistent with the reduced viral loads in the CNS of B6.S mice, suggesting that preferential viral clearance in B6.S mice may have contributed to the reduced T cell responses. In contrast to the higher IFN-γ responses, there was no detectable IL-17 production by B6.S $CD4^+$ T cells at both 8 and 21 dpi, whereas extremely high levels of IL-17 production by SJL $CD4^+$ T cells were detected in response to SP and NSP epitopes at both time points. Notably, the IL-17 levels produced by SJL $CD4^+$ T cells were greater at 21 dpi, which is close to the onset of clinical disease development. These results suggest that the production of high levels of protective IFN-γ in the absence of pathogenic IL-17 in B6.S mice compared to the opposite in SJL mice may provide preferential protection from developing TMEV-induced demyelinating disease.

Unlike SJL DCs, B6.S DCs support viral replication poorly similar to B6 DCs. It has previously been shown using bone marrow chimeras between resistant B10.S and susceptible SJL mice that hematopoietic cells exert a major effect on susceptibility to TMEV (25). We have also confirmed the role of hematopoietic cells in B6.S and SJL mice (data not shown). Because bone-marrow-derived cells affect viral load levels and T cell development in TMEV-infected mice, we characterized the bone-marrow-derived dendritic cells (DCs) of susceptible SJL, resistant B6, and B6.S mice. First, we compared the levels of viral replication in these DCs by detecting viral proteins using flow cytometry after *in vitro* infection with TMEV (Fig. 5). When the DCs were infected with various doses of TMEV for 12 h, the proportion of SJL DCs stained with anti-TMEV antibody was low (1.8%) but detectable after infection with a low (MOI of 0.1) viral concentration (Fig. 5A). The proportions of TMEV-positive SJL DCs increased to 4 to 6% and 30 to 40% after infection at MOI of 1 and 10, respectively. In contrast, no detectable increase in TMEV-positive B6 or B6.S DCs over the uninfected control DCs was observed after infection at an MOI of 0.1. Even at the higher doses of viral infection, only very low levels (1.1% and 2.4% at an MOI of 1 and 3.8% and 6.2% at an MOI of 10, respectively) of TMEV-positive B6 or B6.S DCs were observed. We have previously shown that DCs and other glial cell types from resistant mice poorly support viral replication and spread compared to those from susceptible mice in the comparisons of viral titers and viral protein production (15, 23, 26, 27). These results indicate that DCs from resistant B6 and B6.S mice are less permissive to TMEV infection than DCs from susceptible SJL mice.

To further determine whether the poor support for viral infection and/or replication reflects a time-delayed phenomenon, we infected DCs with a high viral dose (MOI of 10) for various time

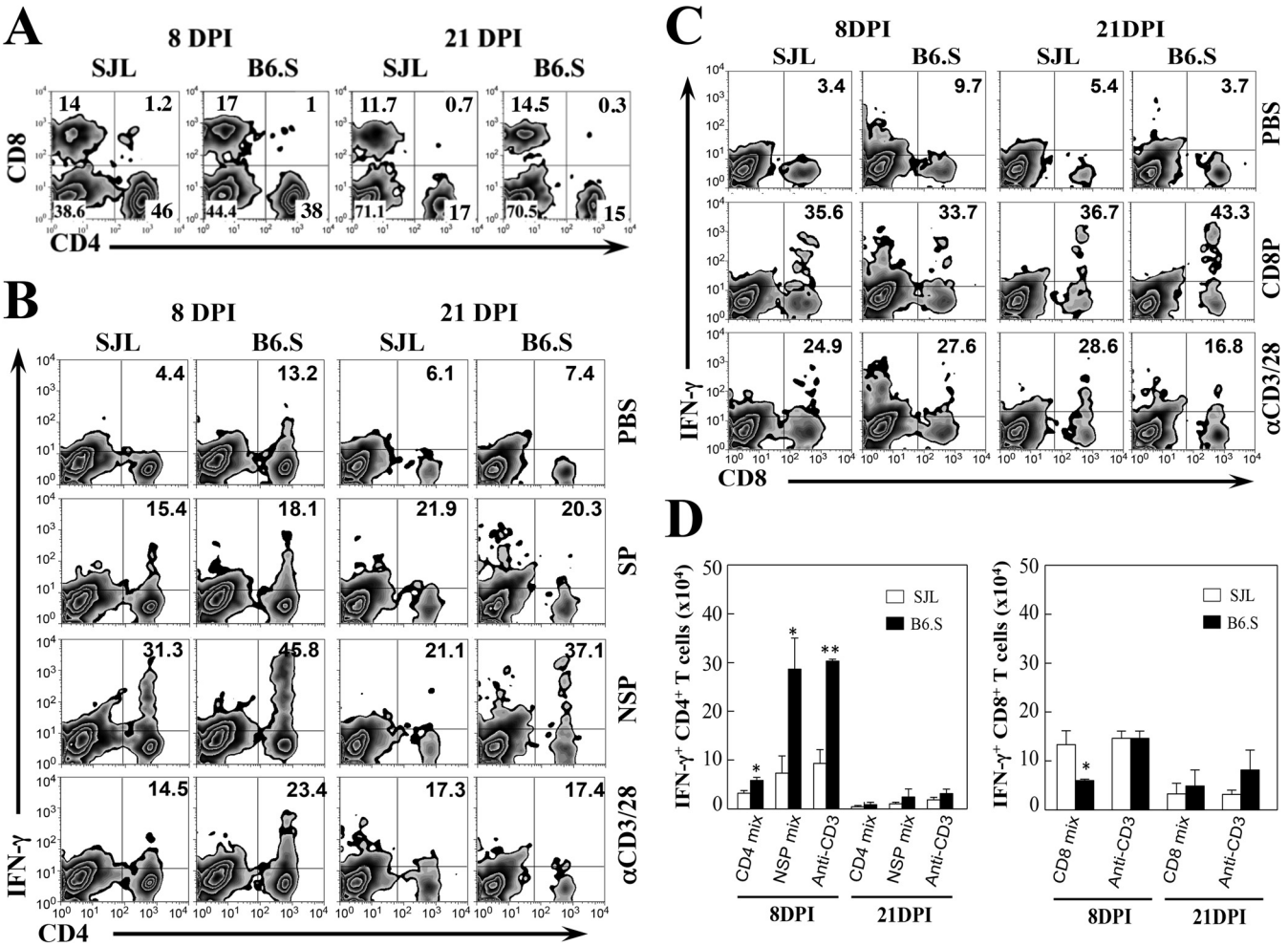

FIG 3 $CD4^+$ and $CD8^+$ T cell responses to viral epitopes in TMEV-infected SJL and B6.S mice. (A) Proportions of CNS-infiltrating $CD4^+$ and $CD8^+$ T cells were determined using flow cytometry at 8 and 21 days postinfection (DPI). The numbers in the fluorescence-activated cell sorter (FACS) plots represent the percentages of $CD4^+$ and $CD8^+$ T cells in the total CNS mononuclear cells. (B) The proportion of IFN-γ-producing $CD4^+$ cells in the CNS was analyzed using intracellular staining after stimulation for 6 h with 2 μM *I-A*^{s}-restricted structural capsid epitope peptides (SP: $VP1_{233–250}$, $VP2_{74–86}$, and $VP3_{24–37}$), nonstructural epitope peptides (NSP: $3D_{6–23}$, $3D_{21–36}$, and $3D_{412–430}$), or anti-CD3 and anti-CD28 antibodies. The numbers in the FACS plots represent the percentages of IFN-γ-producing $CD4^+$ cells from the total infiltrating $CD4^+$ cells. Data represent plots from a representative experiment from three independent experiments. (C) The proportions of IFN-γ-producing $CD8^+$ cells in the CNS after stimulation for 6 h with 2 μM CD8 epitope peptides (CD8: $VP3_{159–166}$, $VP3_{173–181}$, and $VP1_{11–20}$) or anti-CD3 and anti-CD28 antibodies are shown. The numbers in the FACS plots represent the percentages of IFN-γ-producing $CD8^+$ T cells from the total infiltrating $CD8^+$ cells. The data represent a representative experiment from three separate experiments using three mice per group. (D) The overall numbers of IFN-γ-producing $CD4^+$ and $CD8^+$ T cells in the CNS of TMEV-infected SJL and B6.S mice at 8 and 21 days postinfection are shown. The data represent combined results from three independent experiments. Statistically significant differences are indicated with asterisks (*, $P < 0.05$; **, $P < 0.01$).

periods (Fig. 5B). A significant increase in the proportion of TMEV-positive cells started to appear in SJL DCs at 6 h postinfection and further increased to over 40% at 24 h postinfection. In contrast, only low proportions (4 to 5%) of TMEV-positive B6.S and B6 DCs began to appear at 12 h postinfection, and the proportions only reached ~10% at 24 h postinfection. The proportions did not increase further in these DCs at 48 h postinfection. The differences in the viral infections in SJL and B6 DCs were consistent with those from previous reports (15, 23, 27). In addition, the differences in the viral infections between SJL and B6S (41% ± 4.5% versus 8.4% ± 3.1%) are significant and highly reproducible, as shown in the panel where MOI = 10 in Fig. 5A and the panel representing 24 h in Fig. 5B. These data strongly suggest that the level of viral infection and/or replication in B6.S DCs is lower than that in SJL DCs, similar to B6 DCs. Therefore, it is most likely that the levels of various responses to TMEV infection in the major antigen-presenting DCs would be drastically different between B6.S and SJL mice, despite the identical MHC-restricted antigen presentation.

Virus-infected B6.S DCs induce reduced Th17 development compared to SJL DCs. We first compared the ability of DCs from SJL and B6.S mice to induce cognate $CD4^+$ T cell proliferation using purified $CD4^+$ T cells from SJL VP2-TCR-Tg mice. $CD4^+$ T cells from VP2-TCR-Tg mice specifically recognize the TMEV $VP2_{74–86}$ capsid region (18). Purified $CD4^+$ T cells from VP2-TCR-Tg mice were labeled with carboxyfluorescein succinimidyl ester (CFSE) and stimulated with DCs for 4 days in the presence of PBS, $VP2_{74–86}$ peptide, UV-inactivated TMEV (UV-TMEV), infectious low-pathogenicity variant M2 virus, or infectious pathogenic TMEV (Fig. 6A). $CD4^+$ T cell proliferation was determined

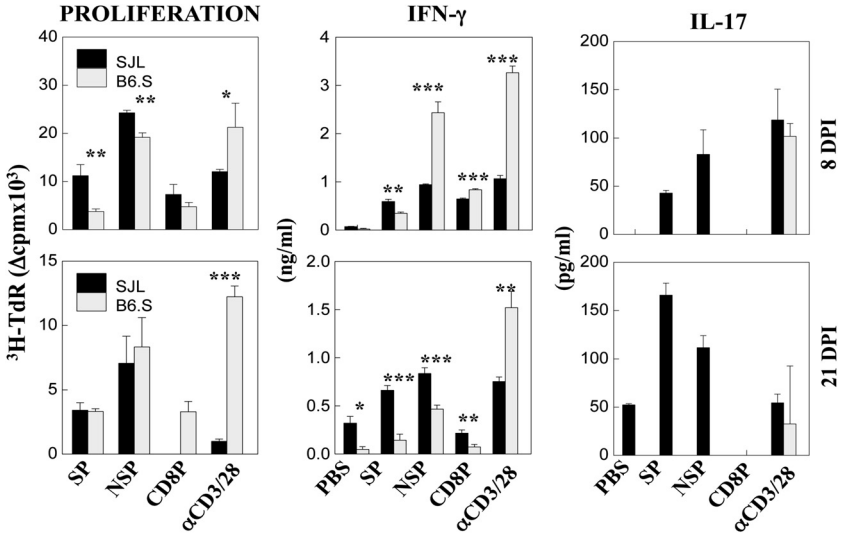

FIG 4 Peripheral T cell responses to TMEV epitopes in TMEV-infected SJL and B6.S mice. Proliferative responses and cytokine production levels (IFN-γ and IL-17) by splenic T cells from mice at 8 and 21 days postinfection were determined following stimulation for 2 days with 2 μM the indicated epitope peptides. Cytokine levels in the culture supernatants were assessed with specific ELISAs. Triplicate analyses of a single representative experiment from three separate experiments are shown. The values represent the mean ± standard deviation of results from triplicate cultures. Statistically significant differences are indicated with asterisks (*, $P < 0.05$; **, $P < 0.01$; ***, $P < 0.001$).

based on the intensity of CFSE, which is lower in proliferating cells. The results clearly indicate that CD4$^+$ T cell proliferation was induced equally well by SJL and B6.S DCs in the presence of all of the stimulants containing the VP2$_{74-86}$ epitope, including UV-TMEV, compared with DCs treated with PBS (mock). Therefore, DCs from B6.S and SJL mice are equally capable of driving cognate CD4$^+$ T cell proliferation with these various forms of stimulants.

We have previously shown that TMEV-infected APCs from resistant B6 mice induce low levels of Th17 development *in vitro* compared to those from susceptible SJL mice (18). However, it was difficult to assess the underlying mechanisms because of the differences in the MHC restriction and consequent T cell repertoires between B6 and SJL mice. Thus, we further compared the levels of Th1/Th17 cell differentiation from the identical VP2-TCR CD4$^+$ T cells in the presence of viral antigen-loaded SJL and B6.S DCs using flow cytometry (Fig. 6B). After activation of VP2$_{74-86}$-specific transgenic CD4$^+$ T cells from VP2-TCR-Tg SJL mice with SJL or B6.S DCs in the presence of VP2$_{74-86}$ peptide, UV-inactivated TMEV, low-pathogenicity variant M2 TMEV (28), or various concentrations of infectious pathogenic TMEV for 4 days, cells were restimulated for 6 h with PMA and ionomycin and analyzed using flow cytometry after staining for intracellular IFN-γ and IL-17. VP2$_{74-86}$ peptide-pulsed, UV-TMEV-pulsed, and low-pathogenicity M2-infected DCs from both mouse strains failed to induce significant Th17 development, while they vigorously induced IFN-γ-producing Th1 cells. In contrast, Th17 cell development was preferentially increased only after stimulation with pathogenic TMEV-infected SJL DCs in a TMEV dose-dependent manner (2 to 30% at MOI of 1 to 10). The Th17 cell development after stimulation with virus-infected B6.S DCs was significantly lower (1 to 11% at MOI of 1 to 10). The differential increase in the Th17 cell development between SJL and B6S DCs infected with TMEV was highly reproducible; e.g., the proportions of Th17 cells in the presence of TMEV-infected DCs (MOI of 10) in Fig. 6B, C, and D were significantly higher than those in the presence of uninfected DCs (26.3% ± 3.2% versus 7% ± 3.6%). These results suggest that stimulation of CD4$^+$ T cells with DCs infected with pathogenic virus preferentially promotes the development of pathogenic Th17 cells.

Because SJL DCs support TMEV replication and Th17 development severalfold higher than those of B6.S DCs (Fig. 5), we further tested the potential role of IL-6 produced by DCs during the T cell stimulation (Fig. 6C and D). Treatment with neutralizing antibodies to IL-6 in these cocultures stimulated with pathogenic TMEV abrogated the Th17 development (Fig. 6C), as shown previously (18). These results suggest that IL-6 production by virus-infected DCs from both mouse strains is associated with Th17 cell differentiation. Addition of IL-17 to the cocultures of VP2-TCR-Tg CD4$^+$ T cells and TMEV-infected DCs enhanced the Th17 development (Fig. 6D), suggesting amplification effects of IL-17 in the Th17 development. Notably, the enhancing effects of IL-17 were abrogated in the presence of IL-6-neutralizing antibodies (Fig. 6D). Taken together, these results strongly suggest that the amplification effect of IL-17 on Th17 development is mediated by IL-17-induced IL-6 production.

TLR-mediated DC stimulation mimics Th17 development by virus-infected DCs. We have previously reported that treatment of DCs from B6 mice with the TLR4 ligand LPS enhanced the induction of Th17 cells via elevated IL-6 production (18). In addition, we also previously demonstrated that signaling via TLR3 and TLR2 is associated with TMEV infection and the consequent production of innate cytokines, including IL-6 (29–31). Therefore, we further examined the effects of various TLR ligands on Th17 development by SJL and B6.S DCs (Fig. 7). VP2-TCR-Tg CD4$^+$ T cells were stimulated with SJL and B6.S DCs loaded with different forms of viral antigens (VP2 peptide, UV-TMEV, and infectious TMEV) in the presence or absence of various TLR agonists: Pam (TLR2 ligand), LTA (TLR2 ligand), poly(I:C) (TLR3 ligand), LPS (TLR4 ligand), CL087 (TLR7 ligand), and CpG (TLR9 ligand). Consistent with previous data

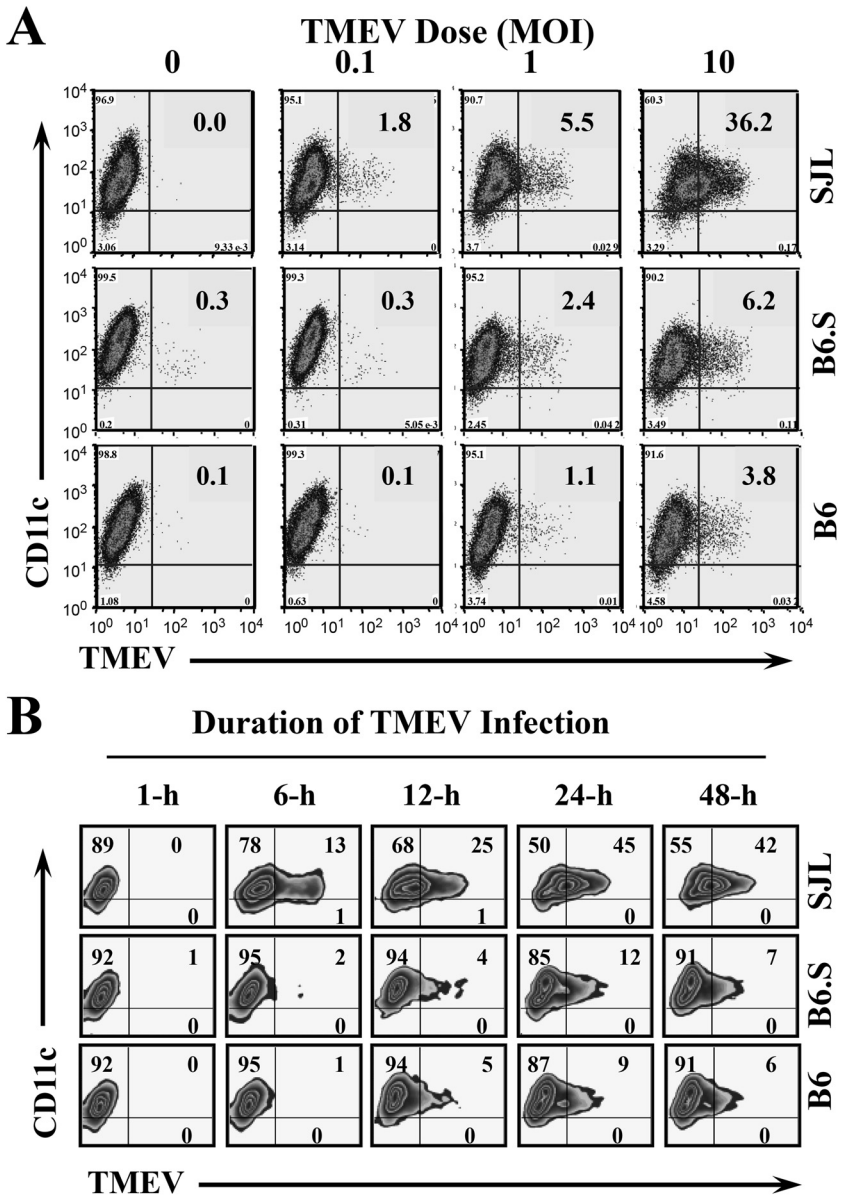

FIG 5 Viral replication levels in DCs derived from SJL, B6.S, and B6 mice after *in vitro* TMEV infection. (A) DCs from B6, B6.S, and SJL mice were infected at an MOI of 0, 0.1, 1, or 10 for 12 h. (B) DCs from B6, B6.S, and SJL mice were infected at MOI of 10 for 1, 6, 12, 24, or 48 h. Expression of TMEV proteins was detected with anti-TMEV and anti-CD11c antibodies using FACS analysis. The numbers in the FACS plots represent the percentage of $TMEV^+$ cells from $CD11c^+$ cells. The results represent a representative experiment of three separate experiments using three mice per group.

(Fig. 6B), $VP2_{74-86}$ peptide- and UV-TMEV-pulsed SJL and B6.S DCs failed to induce Th17 development but not Th1 development. However, $VP2_{74-86}$ peptide- and UV-TMEV-pulsed SJL and B6.S DCs were able to stimulate Th17 development equally well in the presence of certain TLR ligands. The DCs treated with the ligands for TLR2, TLR3, TLR4, and TLR7 induced Th17 development significantly and further increased Th1 development, suggesting that signaling functions for the TLRs are similar in these DCs. The upregulated Th17 development in the presence of TLR3 and TLR4 ligands was consistent with the previous reports (18, 31). In addition, the effects of a given TLR were consistent with the different TMEV-specific stimulants, such as VP2 peptide, UV-TMEV, and TMEV. Interestingly, the TLR9 ligand CpG, which constitutes a bacterial ligand, further promoted Th1 development but failed to stimulate Th17 development. Because these TLRs (TLR2, -3, -4, and -7) are known to be associated with certain bacterial and viral infections, only select TLR-mediated stimulation may affect the development of Th17 cells.

In contrast to the similar Th17 cell development in the presence of DCs loaded with $VP2_{74-86}$ peptide or UV-TMEV in the presence of the select TLR ligands, TMEV-infected SJL DCs in the presence of the TLR ligands, except CpG, induced greater than 2-fold-higher levels of Th17 cells than TMEV-infected SJL DCs in the absence of the TLR ligands. However, virus-infected B6.S DCs consistently induced lower levels of Th17 development in the ab-

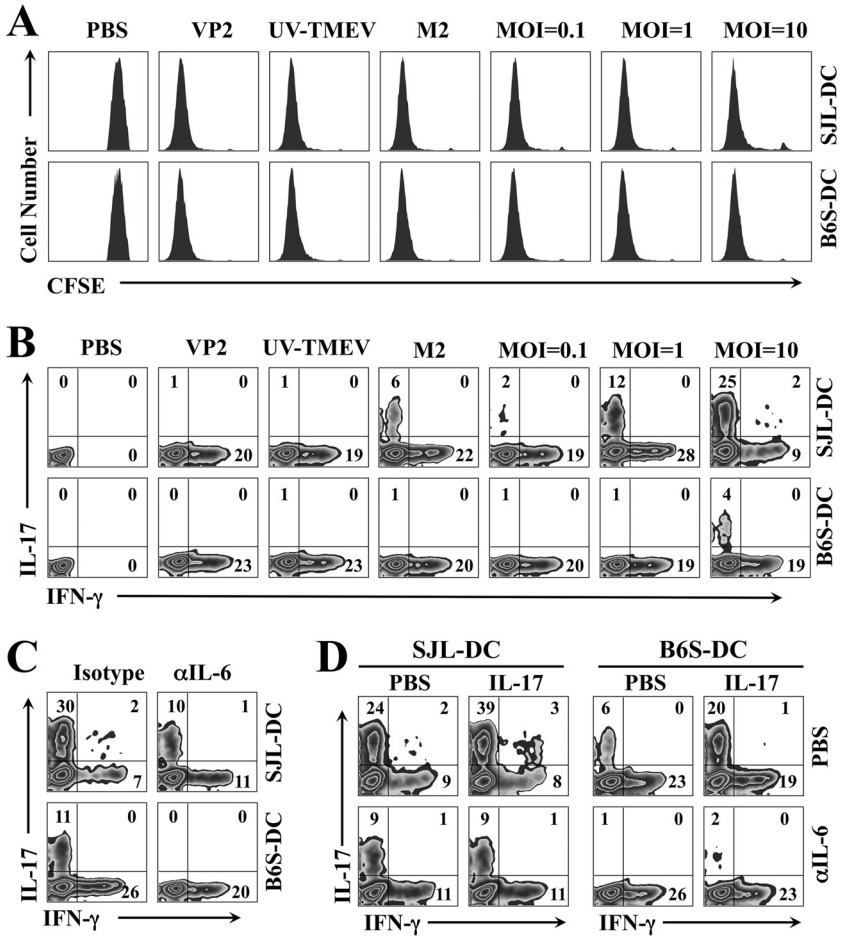

FIG 6 Levels of Th1 and Th17 cell development after stimulation with SJL and B6.S DCs. (A) Purified $CD4^+$ T cells from VP2-TCR-Tg SJL mice were labeled with CFSE and stimulated with SJL or B6.S DCs for 4 days in the presence of PBS, $VP2_{74-86}$ peptide, UV-TMEV, low-pathogenicity variant M2 virus, or pathogenic TMEV. T cell proliferation was analyzed by flow cytometry based on CFSE intensity. (B) $CD4^+$ T cells from VP2-TCR-Tg SJL mice were activated with the stimuli described above and SJL or B6.S DCs for 4 days. Cells were restimulated for 6 h with 50 ng/ml PMA and 1 ng/ml ionomycin and then analyzed using flow cytometry after intracellular staining for IFN-γ and IL-17 cytokines. (C) $CD4^+$ T cells from VP2-TCR-Tg SJL mice were activated for 4 days with TMEV-infected SJL or B6.S DCs in the presence of an isotype control or anti-IL-6 antibody. Cells were then restimulated for 6 h with PMA and ionomycin prior to flow cytometry. (D) $VP2_{74-86}$-specific transgenic $CD4^+$ T cells were activated with TMEV-pulsed SJL or B6.S DCs (MOI of 10) with or without 100 ng/ml IL-17 and PBS or anti-IL-6 antibody for 4 days. The cells were restimulated for 6 h with PMA and ionomycin. All plots were gated on $CD4^+$ T cells, and the numbers in the FACS plots represent the percentages of IFN-γ^+ and IL-17^+ cells within the $CD4^+$ cells. The presented data are representative of three independent experiments.

sence or presence of TLR ligands than infected SJL DCs, although the presence of TLR ligands further elevated Th17 development. Therefore, the level of TMEV replication in SJL and B6.S DCs appears to play a critical role in the development of Th17 cells. It is interesting to note that TMEV infection of SJL DCs in the presence of the TLR9 ligand CpG abrogated the vigorous development of Th1 cells. In contrast, TMEV infection of B6.S DCs in the presence of CpG completely abrogated the development of Th17 cells, leading to only Th1 development. Thus, these results suggest that the innate immunity signals induced following exposure to infectious agents are interactive, and the combinations of these signals may result in various outcomes for the development of Th1 versus Th17 cells.

DISCUSSION

The capability to generate a strong immune response is critical for host survival from infections with various pathogens (32, 33). However, many pathogenic viruses can elude immune responses by multiple strategies, such as alterations in antigen processing, presentation of processed antigen on MHCs, cell apoptosis, and innate cytokine responses (34). Infection of resistant mice with TMEV is successfully cleared in mice with strong early phase protective T cell responses, in contrast to susceptible mice displaying weak early phase immune responses. As a consequence, viral persistence in susceptible mice eventually leads to the development of chronic demyelinating disease (35). Levels and/or qualities of T cell immune responses are associated with the development of TMEV-induced demyelinating disease (15). Studies with different inbred mouse strains showed that one of the most important susceptibility loci is linked to the MHC *H-2D* gene (4–6). Studies using transgenic expression of $H\text{-}2D^b$ in susceptible FVB mice demonstrated the importance of MHC, as the expression of transgene in susceptible mice rendered them resistant (14, 36). Human multiple sclerosis (MS) and experimental autoimmune encepha-

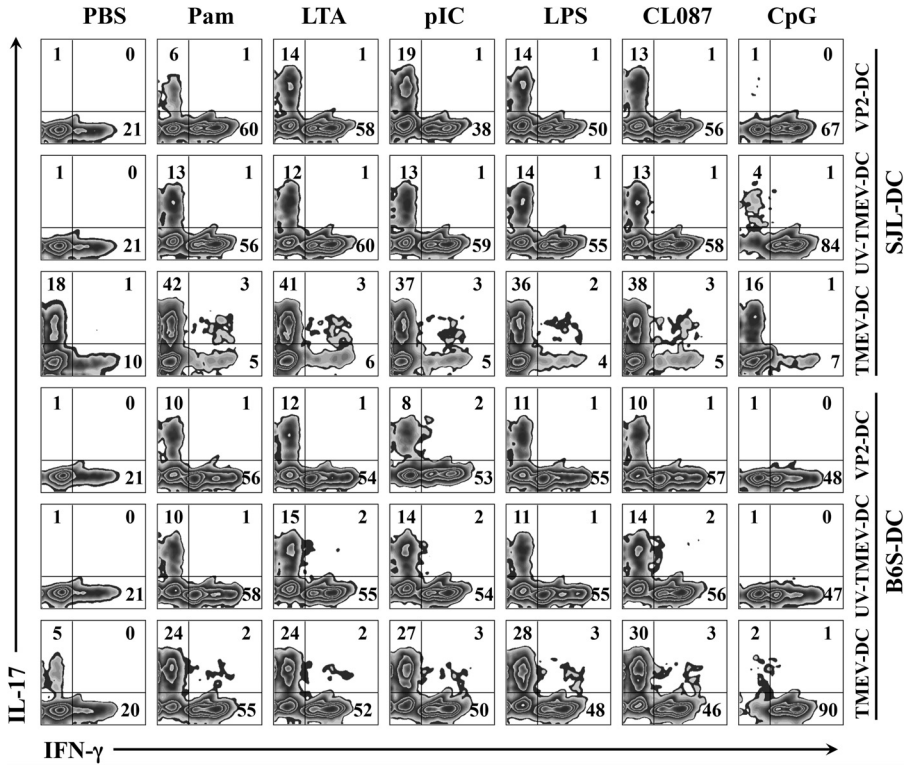

FIG 7 Levels of Th1 and Th17 cell development after stimulation with SJL and B6.S DCs in the presence of various TLR ligands. Purified $CD4^+$ T cells from VP2-TCR-Tg SJL mice were activated for 4 days with SJL or B6.S DCs in the presence of PBS, $VP2_{74-86}$ peptide, UV-TMEV, or live TMEV with or without TLR agonists: Pam3CSK4 (Pam) (TLR2 ligand; 10 ng/ml), LTA (TLR2 ligand; 1 μg/ml), poly(I:C) (TLR3 ligand; 50 μg/ml), LPS (TLR4 ligand; 100 ng/ml), CL087 (TLR7 ligand; 0.1 μg/ml), or CpG (TLR9 ligand; 0.1 μg/ml). The cells were then restimulated for 6 h with PMA and ionomycin prior to FACS analysis. The plots were gated on $CD4^+$ T cells. The numbers in the FACS plots represent the percentages of IFN-γ^+ and IL-17^+ cells within the $CD4^+$ cells. The presented data are representative of two separate experiments.

litis (EAE) models have also shown that susceptibility is strongly associated with MHC haplotypes (37).

However, the B10.S strain from crosses of resistant C57BL/10 mice, which are closely related to prototypically resistant B6 mice, and susceptible SJL mice appear to show conflicting results for viral persistence versus development of demyelinating disease after TMEV infection (4, 10). The level of virus persistence appears to be clearly associated with non-MHC-linked genes located on chromosomes 10, 14, and 18 (9–11). However, the development of disease is somewhat different, depending on the investigators (4, 38). Nevertheless, the underlying mechanisms of viral persistence and susceptibility to the development of disease have not been fully illustrated. Our recent studies suggest that the level of innate immune responses of antigen-presenting cells (APCs), reflecting the degree of initial viral infection and/or replication, may be a critical factor for the development of demyelinating disease (15, 23). APCs from susceptible SJL mice vigorously support the initial viral replication, and the resulting innate cytokines, particularly IL-6 and perhaps type I IFNs, steer the antiviral T cell responses to less protective and more pathogenic types, whereas APCs from resistant B6 mice failed to do the same (15, 18, 23, 24). We hypothesized that B6.S mice, similar to B10.S mice, are relatively resistant to TMEV-IDD due to the poor initial support of viral replication in APCs, which steers away from supporting the pathogenic T cell responses.

Our results in this study clearly indicate that B6.S mice, which share the MHC genes with susceptible SJL mice, are resistant to the development of TMEV-induced demyelinating disease (Fig. 1). The levels of demyelination and axonal damage in B6.S mice were very mild compared to those in SJL mice (Fig. 2). B6.S mice had a higher level of initial viral load in the brain than SJL mice, although lower levels of viral load were maintained in the spinal cord (Fig. 1). It is interesting to note that the early $CD4^+$ T cell response in resistant B6.S mice was predominantly an IFN-γ-producing Th1-type response in the CNS and periphery, whereas in susceptible SJL mice, the T cell response was predominantly IL-17-producing Th17 type (Fig. 3 and 4). These results on T cell responses are consistent with the previous observations in resistant and susceptible mice (15, 18). The differences in the initial $CD4^+$ T cell type may have affected the infiltration of viral loads in the spinal cords and the subsequent pathogenesis, as IL-17 is known to promote viral loads and cellular infiltration as well (18). These data strongly suggest that the MHC is not primarily associated with the induction of $CD4^+$ T cell types, which are the critical factor for the pathogenicity of TMEV.

One of the most important APCs is DC. DCs play a pivotal role in primary T cell responses by presenting antigens to T cells in conjunction with the cognate MHC for the optimum memory responses (39). DCs also play important roles in the pathogenesis of TMEV-IDD by inducing the development of pathogenic Th17 cells (23). It has recently become clear that the overproduction of innate cytokines by APCs following viral infection is associated

with the preferential induction of the Th17 cell-type response and the consequent pathogenesis leading to demyelinating disease (15, 26). However, it is not yet clear what genetic or molecular mechanism plays a critical role in driving naive $CD4^+$ T cells to differentiate into Th17 cells. Our present study demonstrates that the level of viral infection and/or replication in APCs from susceptible SJL mice is high compared to that in APCs from resistant B6.S and B6 mice (Fig. 5). These results indicate that the initial viral infection rate in APCs is controlled by a gene or genes independent from the MHC. The differences in the initial viral load in APCs most likely affect the production of innate cytokines, such as IL-6, which is closely involved in the Th17 polarization (Fig. 6). Several candidate genes have been associated with the differences in the viral loads or the persistence of TMEV (40–42). However, it is not clear whether these candidate genes are also associated with the initial viral infection and/or replication in APCs shown *in vitro* (Fig. 5), because viral persistence in animals may represent more complex consequences of the initial viral loads and viral clearance by the immune response.

Our results further suggest that the initial viral loads in APCs trigger the corresponding levels of innate cytokine production via pathogen recognition receptors. The quantity and quality of adaptive immune responses are determined by the initial innate immune responses (43, 44). The development of the pathogenic Th17 cell type is orchestrated by cytokines, such as transforming growth factor β (TGF-β), IL-6, and IL-23 (45). Our present study (Fig. 7) showed that the Th17 polarization can be achieved equally well in APCs from susceptible and resistant mice with agonists of multiple TLR receptors (TLR2, -3, -4, and -7), which are either known or suspected to be associated with the innate immune responses following TMEV infection (18, 26, 29–31). Therefore, the potential deficiency of the signal induction in any of these TLRs is unlikely to be associated with the differential Th17 polarization. Remarkably, viral infection of APCs in the presence of TLR agonists resulted in further differential increases in Th17 development between susceptible and resistant APCs (Fig. 7), reflecting the differences in the level of viral infection and/or replication (Fig. 5). Taken together, these results strongly suggest that the level of initial viral infection and/or replication in APCs, which is controlled by a MHC-unlinked gene or genes, is the critical factor for the pathogenesis of immune-mediated TMEV-induced demyelinating disease in the CNS. It is also interesting to note that the resistance mechanism of the immune response in F1 between resistant B6 and susceptible SJL mice differs from that of B6.S mice in regard to the type and MHC recognition by the virus-specific T cells (15).

The TCR-Vβ locus, the carbonic anhydrase 2 enzyme locus, a gene close to the IFN-γ locus, and *Tmevp3*, a locus near IL-22, have been proposed for controlling TMEV-induced demyelinating disease (7, 8, 41). Most recently, an enhancer-like long noncoding RNA termed NeST within *Tmevp3* appears to be causal for TMEV (DA strain) persistence in infected mice (42). The SJL/J-derived NeST in transgenic mice conferred increased IFN-γ production in $CD8^+$ T cells and increased Theiler's virus persistence. However, it is unclear at this time whether this locus also confers higher viral infection and replication in APCs *in vitro*. In addition, the increased IFN-γ production by $CD8^+$ T cells in SJL mice may not be universal in TMEV infection, because lower IFN-γ production in SJL mice was observed after infection with the TMEV BeAn strain (15). Furthermore, this locus does not appear to affect the induction of $CD4^+$ T cell types, as $CD4^+$ T cells from the NeST-Tg mice do not exhibit any differences in IFN-γ production (42). Further studies may be necessary to confirm whether this locus is also associated with the altered viral infection and replication in APCs *in vitro*.

ACKNOWLEDGMENT

This work was supported by a research grant (RG 4001-A6) from the National Multiple Sclerosis Society.

REFERENCES

1. **Dal Canto MC, Lipton HL.** 1975. Primary demyelination in Theiler's virus infection. An ultrastructural study. Lab Invest **33:**626–637.
2. **Lipton HL, Dal Canto MC.** 1976. Chronic neurologic disease in Theiler's virus infection of SJL/J mice. J Neurol Sci **30:**201–207. http://dx.doi.org/10.1016/0022-510X(76)90267-7.
3. **Dal Canto MC, Lipton HL.** 1977. A new model of persistent viral infection with primary demyelination. Neurol Neurocir Psiquiatr **18:**455–467.
4. **Rodriguez M, David CS.** 1985. Demyelination induced by Theiler's virus: influence of the H-2 haplotype. J Immunol **135:**2145–2148.
5. **Clatch RJ, Melvold RW, Miller SD, Lipton HL.** 1985. Theiler's murine encephalomyelitis virus (TMEV)-induced demyelinating disease in mice is influenced by the H-2D region: correlation with TEMV-specific delayed-type hypersensitivity. J Immunol **135:**1408–1414.
6. **Rodriguez M, Leibowitz J, David CS.** 1986. Susceptibility to Theiler's virus-induced demyelination. Mapping of the gene within the H-2D region. J Exp Med **163:**620–631.
7. **Melvold RW, Jokinen DM, Knobler RL, Lipton HL.** 1987. Variations in genetic control of susceptibility to Theiler's murine encephalomyelitis virus (TMEV)-induced demyelinating disease. I. Differences between susceptible SJL/J and resistant BALB/c strains map near the T cell beta-chain constant gene on chromosome 6. J Immunol **138:**1429–1433.
8. **Melvold RW, Jokinen DM, Miller SD, Dal Canto MC, Lipton HL.** 1990. Identification of a locus on mouse chromosome 3 involved in differential susceptibility to Theiler's murine encephalomyelitis virus-induced demyelinating disease. J Virol **64:**686–690.
9. **Bureau JF, Montagutelli X, Lefebvre S, Guenet JL, Pla M, Brahic M.** 1992. The interaction of two groups of murine genes determines the persistence of Theiler's virus in the central nervous system. J Virol **66:**4698–4704.
10. **Bureau JF, Montagutelli X, Bihl F, Lefebvre S, Guenet JL, Brahic M.** 1993. Mapping loci influencing the persistence of Theiler's virus in the murine central nervous system. Nat Genet **5:**87–91. http://dx.doi.org/10.1038/ng0993-87.
11. **Bureau JF, Drescher KM, Pease LR, Vikoren T, Delcroix M, Zoecklein L, Brahic M, Rodriguez M.** 1998. Chromosome 14 contains determinants that regulate susceptibility to Theiler's virus-induced demyelination in the mouse. Genetics **148:**1941–1949.
12. **Lipton HL, Dal Canto MC.** 1979. Susceptibility of inbred mice to chronic central nervous system infection by Theiler's murine encephalomyelitis virus. Infect Immun **26:**369–374.
13. **Lipton HL, Melvold R.** 1984. Genetic analysis of susceptibility to Theiler's virus-induced demyelinating disease in mice. J Immunol **132:**1821–1825.
14. **Azoulay A, Brahic M, Bureau JF.** 1994. FVB mice transgenic for the H-2Db gene become resistant to persistent infection by Theiler's virus. J Virol **68:**4049–4052.
15. **Jin YH, Kang HS, Mohindru M, Kim BS.** 2011. Preferential induction of protective T cell responses to Theiler's virus in resistant (C57BL/6 × SJL)F1 mice. J Virol **85:**3033–3040. http://dx.doi.org/10.1128/JVI.02400-10.
16. **Pullen LC, Miller SD, Dal Canto MC, Van der Meide PH, Kim BS.** 1994. Alteration in the level of interferon-gamma results in acceleration of Theiler's virus-induced demyelinating disease. J Neuroimmunol **55:**143–152. http://dx.doi.org/10.1016/0165-5728(94)90004-3.
17. **Park H, Li Z, Yang XO, Chang SH, Nurieva R, Wang YH, Wang Y, Hood L, Zhu Z, Tian Q, Dong C.** 2005. A distinct lineage of CD4 T cells regulates tissue inflammation by producing interleukin 17. Nat Immunol **6:**1133–1141. http://dx.doi.org/10.1038/ni1261.
18. **Hou W, Kang HS, Kim BS.** 2009. Th17 cells enhance viral persistence and inhibit T cell cytotoxicity in a model of chronic virus infection. J Exp Med **206:**313–328. http://dx.doi.org/10.1084/jem.20082030.

19. **Dal Canto MC, Kim BS, Miller SD, Melvold RW.** 1996. Theiler's murine encephalomyelitis virus (TMEV)-induced demyelination: a model for human multiple sclerosis. Methods **10:**453–461. http://dx.doi.org/10.1006/meth.1996.0123.
20. **Mohindru M, Kang B, Kim BS.** 2006. Initial capsid-specific CD4(+) T cell responses protect against Theiler's murine encephalomyelitis virus-induced demyelinating disease. Eur J Immunol **36:**2106–2115. http://dx.doi.org/10.1002/eji.200535785.
21. **Delgado S, Sheremata WA.** 2006. The role of CD4+ T-cells in the development of MS. Neurol Res 28:245–249. http://dx.doi.org/10.1179/016164106X98107.
22. **Pullen LC, Park SH, Miller SD, Dal Canto MC, Kim BS.** 1995. Treatment with bacterial LPS renders genetically resistant C57BL/6 mice susceptible to Theiler's virus-induced demyelinating disease. J Immunol **155:**4497–4503.
23. **Hou W, So EY, Kim BS.** 2007. Role of dendritic cells in differential susceptibility to viral demyelinating disease. PLoS Pathog **3:**e124. http://dx.doi.org/10.1371/journal.ppat.0030124.
24. **Hou W, Jin YH, Kang HS, Kim BS.** 2014. Interleukin-6 (IL-6) and IL-17 synergistically promote viral persistence by inhibiting cellular apoptosis and cytotoxic T cell function. J Virol **88:**8479–8489. http://dx.doi.org/10.1128/JVI.00724-14.
25. **Aubagnac S, Brahic M, Bureau JF.** 2002. Bone marrow chimeras reveal non-H-2 hematopoietic control of susceptibility to Theiler's virus persistent infection. J Virol **76:**5807–5812. http://dx.doi.org/10.1128/JVI.76.11.5807-5812.2002.
26. **Jin YH, Mohindru M, Kang MH, Fuller AC, Kang B, Gallo D, Kim BS.** 2007. Differential virus replication, cytokine production, and antigen-presenting function by microglia from susceptible and resistant mice infected with Theiler's virus. J Virol **81:**11690–11702. http://dx.doi.org/10.1128/JVI.01034-07.
27. **Kang MH, So EY, Park H, Kim BS.** 2008. Replication of Theiler's virus requires NF-kappaB-activation: higher viral replication and spreading in astrocytes from susceptible mice. Glia **56:**942–953. http://dx.doi.org/10.1002/glia.20668.
28. **Kim BS, Yauch RL, Bahk YY, Kang JA, Dal Canto MC, Hall CK.** 1998. A spontaneous low-pathogenic variant of Theiler's virus contains an amino acid substitution within the predominant VP1(233-250) T-cell epitope. J Virol **72:**1020–1027.
29. **So EY, Kang MH, Kim BS.** 2006. Induction of chemokine and cytokine genes in astrocytes following infection with Theiler's murine encephalomyelitis virus is mediated by the Toll-like receptor 3. Glia **53:**858–867. http://dx.doi.org/10.1002/glia.20346.
30. **So EY, Kim BS.** 2009. Theiler's virus infection induces TLR3-dependent upregulation of TLR2 critical for proinflammatory cytokine production. Glia **57:**1216–1226. http://dx.doi.org/10.1002/glia.20843.
31. **Jin YH, Kaneyama T, Kang MH, Kang HS, Koh CS, Kim BS.** 2011. TLR3 signaling is either protective or pathogenic for the development of Theiler's virus-induced demyelinating disease depending on the time of viral infection. J Neuroinflammation **8:**178. http://dx.doi.org/10.1186/1742-2094-8-178.
32. **Janeway CA, Jr, Medzhitov R.** 2002. Innate immune recognition. Annu Rev Immunol **20:**197–216. http://dx.doi.org/10.1146/annurev.immunol.20.083001.084359.
33. **Wong P, Pamer EG.** 2003. CD8 T cell responses to infectious pathogens. Annu Rev Immunol **21:**29–70. http://dx.doi.org/10.1146/annurev.immunol.21.120601.141114.
34. **Tortorella D, Gewurz BE, Furman MH, Schust DJ, Ploegh HL.** 2000. Viral subversion of the immune system. Annu Rev Immunol **18:**861–926. http://dx.doi.org/10.1146/annurev.immunol.18.1.861.
35. **Kang HS, Kim BS.** 2010. Predominant clonal accumulation of CD8+ T cells with moderate avidity in the central nervous systems of Theiler's virus-infected C57BL/6 mice. J Virol **84:**2774–2786. http://dx.doi.org/10.1128/JVI.01948-09.
36. **Azoulay-Cayla A, Syan S, Brahic M, Bureau JF.** 2001. Roles of the H-2D(b) and H-K(b) genes in resistance to persistent Theiler's murine encephalomyelitis virus infection of the central nervous system. J Gen Virol **82:**1043–1047.
37. **Luckey D, Bastakoty D, Mangalam AK.** 2011. Role of HLA class II genes in susceptibility and resistance to multiple sclerosis: studies using HLA transgenic mice. J Autoimmun **37:**122–128. http://dx.doi.org/10.1016/j.jaut.2011.05.001.
38. **Rodriguez M, David CS.** 1995. H-2Dd transgene suppresses Theiler's virus-induced demyelination in susceptible strains of mice. J Neurovirol **1:**111–117. http://dx.doi.org/10.3109/13550289509111015.
39. **Granucci F, Foti M, Ricciardi-Castagnoli P.** 2005. Dendritic cell biology. Adv Immunol **88:**193–233. http://dx.doi.org/10.1016/S0065-2776(05)88006-X.
40. **Brahic M, Bureau JF, Michiels T.** 2005. The genetics of the persistent infection and demyelinating disease caused by Theiler's virus. Annu Rev Microbiol **59:**279–298. http://dx.doi.org/10.1146/annurev.micro.59.030804.121242.
41. **Levillayer F, Mas M, Levi-Acobas F, Brahic M, Bureau JF.** 2007. Interleukin 22 is a candidate gene for Tmevp3, a locus controlling Theiler's virus-induced neurological diseases. Genetics **176:**1835–1844. http://dx.doi.org/10.1534/genetics.107.073536.
42. **Gomez JA, Wapinski OL, Yang YW, Bureau JF, Gopinath S, Monack DM, Chang HY, Brahic M, Kirkegaard K.** 2013. The NeST long ncRNA controls microbial susceptibility and epigenetic activation of the interferon-gamma locus. Cell **152:**743–754. http://dx.doi.org/10.1016/j.cell.2013.01.015.
43. **Kawai T, Akira S.** 2011. Toll-like receptors and their crosstalk with other innate receptors in infection and immunity. Immunity **34:**637–650. http://dx.doi.org/10.1016/j.immuni.2011.05.006.
44. **Kawai T, Akira S.** 2010. The role of pattern-recognition receptors in innate immunity: update on Toll-like receptors. Nat Immunol **11:**373–384. http://dx.doi.org/10.1038/ni.1863.
45. **Ivanov II, McKenzie BS, Zhou L, Tadokoro CE, Lepelley A, Lafaille JJ, Cua DJ, Littman DR.** 2006. The orphan nuclear receptor RORgammat directs the differentiation program of proinflammatory IL-17+ T helper cells. Cell **126:**1121–1133. http://dx.doi.org/10.1016/j.cell.2006.07.035.